

Indium adatom diffusion and clustering on stepped copper surfaces

Clinton DeW. Van Sicien

Idaho National Engineering Laboratory, P.O. Box 1625, Idaho Falls, Idaho 83415

(Received 31 May 1994; revised manuscript received 13 December 1994)

The energetics of indium adatom diffusion and clustering on stepped Cu (001) and (111) surfaces are determined by energy minimization calculations using the embedded-atom method. The terrace substitutional site is found to be energetically favored over adatom and bulk sites in each case, contrary to recent molecular-cluster calculations. Incorporation of indium adatoms into surface substitutional sites by an exchange mechanism is unlikely at low temperatures except at one type of close-packed step on the Cu (111) surface. Condensation of indium adatoms into epitaxial clusters with square and trigonal symmetry at (001) and (111) surfaces, respectively, will occur at low temperatures, while clustering of surface substitutional indium atoms will not. The considerable mobility, and subsequent clustering, of terrace substitutional indium atoms inferred from recent perturbed-angular-correlation experiments utilizing ^{111}In as a radioactive probe thus conflict with these calculations.

I. INTRODUCTION

Atomic processes occurring at surfaces are of fundamental interest as well as of technological importance. The basic event is adatom diffusion and subsequent trapping at surface defects.¹ At present, details of individual adatom behavior are accessible only by field ion microscopy² and by scanning tunneling microscopy,³ although the behavior of large populations of adatoms and defects can be ascertained by various surface diffraction techniques.^{4,5} In recent years, the perturbed γ - γ angular correlation (PAC) method, where information about the immediate environment of an implanted probe atom is gained as the probe nucleus decays by correlated emission of two γ particles, has been extended from bulk to surface studies. The PAC method is unique in that it provides a way to unobtrusively monitor the behavior of a very dilute concentration of impurity atoms over a range of temperatures.

The total-energy calculations of indium atoms at various sites on and in Cu (001) and (111) surfaces presented here are motivated by a series of PAC experiments in which ^{111}In was used as the nuclear probe to study the temperature dependence of diffusion and trapping phenomena at several low-index surfaces of Cu,⁶⁻¹⁰ Ag,^{11,12} Ni,¹⁰ and Pd.¹³ Because the measured correlation of the two decay γ particles reflects the coupling of the nuclear quadrupole moment and the electric field gradient (EFG) due to the atomic surroundings, it is sensitive only to the nearest neighbors of the probe atom. The data to be interpreted, then, include the strength of the EFG tensor, usually described by the largest component V_{zz} in the principal-axis system, the asymmetry parameter $\eta = (V_{xx} - V_{yy})/V_{zz}$, and the orientation of the principal-axis system with respect to the laboratory frame.¹⁴

To construct a consistent model of the various trapping sites on Cu (001) and (111) surfaces, the following sequence of PAC experiments was performed. First, Klas *et al.*^{6,8} evaporated 10^{-4} monolayer (ML) of ^{111}In onto

the surface in each case, annealed the sample to a high temperature (400–600 K) to drive off any other adsorbed impurities (principally chlorine), and subsequently detected a single population of probe atoms signifying a distinct local atomic environment. That site was found to have a large EFG ($|V_{zz}| = 10^{18} \text{ V cm}^{-2}$) directed perpendicularly to the surface ($\eta = 0$), and so the indium, “frozen in” at the high annealing temperature, was assumed to occupy terrace substitutional sites (sites within the surface layer of copper atoms).

With the high-temperature equilibrium site thus identified, Klas *et al.*⁸ again evaporated 10^{-4} ML of ^{111}In into a vicinal Cu (111) surface at 77 K, and were able to distinguish separate populations of indium atoms that evolved during a series of isochronal anneals up to 850 K. The initial fraction f_1 , comprised of the indium atoms at a unique trapping site immediately following deposition, declined precipitously during annealing at 140 K as a new fraction f_2 appeared. The latter, in turn, essentially disappeared during the 250 K anneal, and the fraction f_3 , easily identified from the previous work as indium at terrace substitutional sites, appeared. The populations f_1 and f_2 were ascribed to indium adatoms at surface steps and indium atoms at substitutional step sites, respectively, due to the reduced strength of the EFG's, the nonzero values of the corresponding asymmetry parameters, and the correlation of the principal-axis orientations with the step direction. Klas *et al.* thus envisioned the following scenario: “We assume that the ^{111}In probes after deposition at 77 K are still mobile enough to reach nearby steps [which are 8.5 lattice spacings apart] and are trapped as adatoms (f_1). . . . The adatom step site for ^{111}In converts around 140 K into a substitutional step site (f_2) by trapping of a step vacancy. Then at annealing temperatures above 200 K the ^{111}In probes diffuse into the top-most monolayer via vacancy mechanism in order to occupy substitutional terrace sites (f_3).” These assignments of the three observed populations to specific trapping sites on Cu (111) are supported by molecular-cluster cal-

culations by Lindgren¹⁵ giving the EFG's at the ¹¹¹Cd atom (to which ¹¹¹In decays by electron capture) positions within and atop a Cu surface cluster. More recently Schatz *et al.*¹⁶ have reported a population of indium adatoms on Cu (001) terraces at annealing temperatures less than 100 K; the corresponding population on Cu (111) terraces has not yet been detected, presumably due to a very low activation energy for diffusion on that surface.

Because the PAC experiments showed a high sensitivity to probe-impurity configurations (by a detuning of the EFG for the isolated probes), further information on indium diffusion at surfaces was sought by monitoring probe populations perturbed by a low coverage of other impurity adatoms. Klas *et al.*^{7,9} again evaporated 10⁻⁴ ML of ¹¹¹In onto vicinal Cu (001) and (111) surfaces, annealed the samples at high temperature to ensure that all probe atoms occupied terrace substitutional sites, and then evaporated 0.07 and 0.08 ML, respectively, of natural indium onto those surfaces at 77 K. A series of isochronal anneals at increasing temperatures led, in each case, to the appearance of two distinct ¹¹¹In populations in addition to the probe atoms at terrace substitutional sites (referred to below as the fraction f_0). Interestingly, all three populations were characterized by very similar EFG's and very small or zero values for the asymmetry parameter, suggesting that the corresponding trapping sites are all terrace substitutional. In the case of the Cu (001) surface,^{7,9} the initial population f_0 dominated a new population f'_0 immediately following deposition of the natural indium overlayer and during the 150 K anneal. The fraction f_0 then declined precipitously as f'_0 grew rapidly during the anneal at 200 K. The third population f''_0 appeared during the 200 K anneal, increased significantly during the 240 K anneal as the fraction f'_0 decreased, and then increased more slowly during the higher temperature anneals up to 580 K as f'_0 decreased at a similar rate. In a separate experiment, the ¹¹¹In populations were monitored for annealing temperatures increasing from 230 to 520 K, where each temperature was held constant for a period of several hours in order to establish near-equilibrium populations. Between 230 and 470 K, fraction f'_0 increased as f''_0 decreased; at 470 K, f''_0 vanished and f_0 reappeared; above 470 K, f_0 increased while f'_0 decreased.

The populations f'_0 and f''_0 were considered to be ¹¹¹In atoms at terrace substitutional sites with one or more, respectively, natural indium neighbors also located in the surface layer. Thus the growth at 200 K of the fraction f'_0 at the expense of f_0 , and the subsequent growth at 240 K of the fraction f''_0 at the expense of f'_0 , are due to clustering—within the surface layer—of the indium atoms. The opposite sequence of population changes apparent at high temperatures is then due to dissolution of the clusters.

As mentioned above, very similar PAC results were obtained for the case of the Cu (111) surface.⁹ The initial population f_0 of probe atoms at terrace substitutional sites increased significantly during annealing at 170–200 K, from the population evident immediately following deposition of an overlayer of 0.08 ML natural indium at

77 K. Klas *et al.*⁹ ascribed this increase to the breakup of clusters comprised of natural indium adatoms weakly bound to terrace substitutional probe atoms. The fraction f_0 then decreased during the anneals at 240 K and above. The fractions f'_0 and f''_0 both appeared during the 170 K anneal, the former increasing rapidly during subsequent higher temperature anneals but then falling precipitously during the 400 K anneal, and the latter increasing less rapidly but becoming the dominant population at annealing temperatures of 400 K and above.

The PAC results for Cu surfaces described here are qualitatively similar to those reported for other fcc metals.^{10–13,17} What is remarkable is the apparent mobility—even at temperatures well below room temperature—of ¹¹¹In atoms *within* the Cu surface layer. At approximately 200 K, step substitutional probe atoms begin to diffuse into the surface layer, and indium clusters begin to form within the surface layer.

The improbability of this phenomenon was recognized by Li *et al.*,¹⁸ who performed molecular-cluster calculations to determine the equilibrium site of the indium atom at a Cu (001) surface and the EFG's characterizing that and alternative sites. Contrary to (the interpretation of) the PAC results, they found the adatomic fourfold-coordinated equilibrium site to be energetically favored (by about 0.5 eV) over the terrace substitutional site. Like Lindgren,¹⁵ they found the EFG at the Cd adatomic site to be considerably smaller than that at the Cd terrace substitutional site. In addition, clusters of two Cd atoms at adjacent terrace substitutional sites produced asymmetry parameters η very close to unity, rather than zero as obtained by PAC in the indium clustering experiments. To reconcile their calculations with the PAC results, Li *et al.* speculated that the populations f'_0 and f''_0 were two-layer indium clusters comprised of single ¹¹¹In atoms at terrace substitutional sites trapping one or several natural indium adatoms. They did not, however, calculate the corresponding EFG's to compare with experiment.

Taken together, the research described above presents a rather confusing picture of indium diffusion and clustering on Cu surfaces. The PAC results are unambiguous and allow a consistent description of events at the Cu (001) and (111) surfaces, but seem to require easy incorporation of indium adatoms into the surface layer and remarkable mobility of indium atoms within the surface layer. Because the probe atoms occupy terrace substitutional sites at the highest annealing temperatures, those sites are energetically favored at low temperatures as well, thus apparently precluding diffusion of substitutional indium over the surface by an exotic “exchange” mechanism. Furthermore, indium clustering within the surface layer is inconsistent with the view of indium as an “oversized” impurity in copper (atomic radius 1.67 and 1.28 Å, respectively¹⁹). The conclusions of Li *et al.* seem to defy intuition as well: One would expect that the low-temperature equilibrium site for an indium atom would be at the Cu surface, since indium is nearly insoluble in copper at low temperatures,²⁰ but within rather than above the Cu surface layer in order to maximize the num-

ber of In-Cu bonds. It seems unlikely that their indium adatom clusters tethered to terrace substitutional probe atoms would survive at the high annealing temperatures of the PAC experiments, or that a probe atom so buried would experience the large EFG's found experimentally.

It is thus important to evaluate theoretically the energetics of indium atoms and clusters at stepped Cu (001) and (111) surfaces in order to project their behavior at the PAC annealing temperatures. Because surface reconstruction, structural relaxation about the impurity atom(s), surface steps and kinks, etc., greatly reduce the symmetry of the system, and because many indium sites and configurations must be considered, *ab initio* and molecular-cluster calculations are not feasible. The total-energy calculations presented below use the computationally efficient, semiempirical embedded-atom method (EAM) of Daw and Baskes,²¹ chosen in part because the copper description produced by the EAM procedure is so well characterized in the literature.

II. ENERGETICS CALCULATIONS

A. Theoretical method

The embedded-atom method for calculating the total energy of a system of atoms is based on the idea that the cohesive energy of a metallic system can be expressed in terms of "embedding" energies. The embedding energy is the potential energy gained when an atom is embedded into the local electron density provided by the remaining atoms of the system, and so includes many-body interactions. The ansatz given by Daw and Baskes²¹ for the total (cohesive) energy is

$$E_{\text{coh}} = \sum_i G_i \left[\sum_{j \neq i} \rho_j^a(r_{ij}) \right] + \frac{1}{2} \sum_{i,j (j \neq i)} U_{ij}(r_{ij}), \quad (1)$$

where the embedding energy G_i for an atom i is a functional of the electron density at site i produced by the spherically averaged atomic electron densities ρ_j^a centered on the surrounding atoms j , U is an electrostatic pair interaction describing the screened internuclear repulsion, and r_{ij} is the distance between the centers of atoms i and j . A consistent set of the G_i and U_{ij} must be found for application to a specific system.

The procedure for obtaining such a consistent set for a pure metal or alloy is outlined by Foiles, Baskes, and Daw,²² and indeed the function set for Cu used in the present work is taken from that paper. The EAM description of Cu reproduces exactly the lattice constant, sublimation energy, and bulk modulus, due to the fitting requirement that the cohesive energy as a function of lattice constant follow the "universal binding curve" of Rose *et al.*²³ This set of embedding functions and pair interactions for Cu was derived in conjunction with sets for the transition metals Ag, Au, Ni, Pd, and Pt, such that the fitted values for the elastic constants, the vacancy formation energies, and the dilute heats of mixing for the binary alloys match the experimental values reasonably well. Surface reconstruction²² and surface phonon modes²⁴ calculated with this particular EAM description

of Cu compare very well with the corresponding experimental values available. [But note that Liu *et al.*²⁵ and Tian and Rahman²⁶ have shown that this description does not favor self-diffusion on Cu (001) by the exchange process over the bridge "jump" process, contrary to what may occur experimentally.⁵] Liu and Adams²⁷ and Tian and Rahman²⁶ have recently reported detailed EAM studies of the energetics of stepped Cu (001) surfaces.

Ideally, a new, consistent set of embedding functions and pair interactions would be found to describe Cu and In, by fitting to their elemental and alloy bulk properties. However, the structure of the δ phase containing 30 at. % indium, which is the only alloy phase stable at low temperatures, is controversial.²⁰ Thus a function set for indium was derived by fitting to indium bulk properties and to the heat of formation of dilute indium in copper, while using the function set for copper provided by Foiles, Baskes, and Daw²² as discussed above. It is felt that the set for copper is both "optimized" and versatile due to the large number of fitting parameters involving other transition metals that it satisfies, and that the use of *dilute* alloy properties to generate the indium set is reasonable for a study of indium diffusion at surfaces. Alternatively, one could obtain an indium function set by fitting to *ab initio* total-energy calculations for varying lattice parameters of the pure In lattice and a Cu-In alloy. Breeman and co-workers^{28,29} have recently reported embedded-atom-type calculations for indium atoms at the Cu (001) surface using the Finnis-Sinclair model³⁰ with the indium potential parameters found in this manner.

For the purposes of this work, face-centered-tetragonal indium (axial ratio $c/a=1.076$) was treated as face-centered cubic with lattice constant $a=4.71$ Å to preserve the volume of the tetragonal unit cell. Interestingly, Yokozeki and Stein³¹ have shown that unsupported pure indium clusters smaller than 5 nm diameter have the fcc structure with that volume-preserving lattice constant. The indium sublimation energy of 2.5212 eV/atom was taken from the tables of Kubaschewski, Evans, and Alcock.³² The bulk modulus B used was 402 kbar at 0 K, as calculated by Varotsos³³ from the experimental data of Flower, Saunders, and Yögürçü³⁴ taken at room temperature. These quantities are reproduced exactly due to use of the cohesive energy-lattice constant relation found by Rose *et al.*²³

The fitting parameters were then varied so that the indium function set would reproduce the experimental values for the Poisson ratio ν and the vacancy formation energy in bulk In, the heat of formation of dilute indium in Cu, and, additionally, the heat of formation of dilute indium in Ag [using the EAM function set for Ag (Ref. 22)]. The "isotropic" Poisson ratio of 0.43 was calculated using the compliance matrix S provided by Simmons and Wang³⁵ for a fct indium single crystal, but setting $\nu = -S'_{12}/S'_{11}$ rather than $-S_{12}/S_{11}$, where $S'_{12} = (S_{12} + S_{13})/2$ and $S'_{11} = (S_{11} + S_{11} + S_{33})/3$. (Note that all elastic properties of an isotropic body are fixed by specifying B and ν .) The vacancy formation energy was taken to be 0.50 eV, which is an average of a range of values from 0.45 to 0.57 eV obtained by positron annihi-

lation spectroscopy (Varotsos³³ and Seeger³⁶). The heats of formation of dilute indium in Cu and in Ag were determined calorimetrically at 723 K by Kleppa to be 0 eV (Ref. 37) and -0.421 eV (Ref. 38), respectively; these are expected to be little changed at 0 K. (Jacob and Alcock³⁹ and Bhattacharya and Masson⁴⁰ have commented on Kleppa's work.)

The "best fit" parameters values were found to be $n_s = 1.42011$ and $n_p = 1.57989$ in the parametrized expression²² for the indium atomic electron density and $Z_0 = 3$, $\alpha = 2.13618$, $\beta = 7.00215$, and $\nu = 2$ in the expression²² for the indium effective charge used to define the repulsive pair interaction. The interaction cutoff distance was taken to be 6.5 \AA .

The utility of this semiempirical, EAM description of indium depends, of course, on the degree to which calculated values match experimental values. The (attractive) binding energy for a substitutional In-vacancy defect in Cu is found to be -0.18 eV, which is to be compared with values $-0.29(6)$ eV calculated from positron annihilation Doppler-broadening measurements (Bosse *et al.*⁴¹ and Lühr-Tanck *et al.*⁴²), -0.26 eV determined from PAC measurements (Pleiter and Hohenemser⁴³), and -0.25 eV obtained by analysis of diffusion data (quoted by Benedek⁴⁴). The (attractive) binding energy for a substitutional In-interstitial Cu defect⁴⁵ in Cu is found to be -0.32 eV, which is identical to the value determined from resistivity recovery measurements by Wollenberger.⁴⁶ It should be noted that the EAM calculations are performed at 0 K and so give the binding enthalpy, while the experiments give the Gibbs binding free energy.

B. Atomic indium at surfaces

The Cu slabs for which the total-energy calculations were made consist of 17 layers, each comprised of 288 Cu atoms, with the top layer a free surface and the atoms in the bottom four layers held fixed at their bulk lattice positions. The slab periodicity in directions transverse to the surface normal was kept constant, while allowing surface reconstruction and local atomic relaxation around surface defects. For both Cu (001) and (111) surfaces, only steps in the close-packed $\langle 110 \rangle$ -type directions (which have the lowest energy), and one atomic layer high, were considered. The surface dimensions were changed (from square to rectangular) when necessary to minimize interactions between periodically repeated defects. As in all molecular statics calculations, the total, relaxed energy of the collection of Cu and In atoms was found by moving the atoms about to minimize the forces

TABLE I. Formation energy (eV) for indium at or near the Cu (001) or (111) surface, relative to that for indium in the bulk.

Layer number (from surface)	Crystallographic surface	
	(001)	(111)
Adatomic site	-0.39	-0.21
1	-0.82	-0.62
2	-0.16	-0.09
3	-0.01	-0.01
4	0.00	0.00

TABLE II. Binding energy (eV) of indium atoms at stepped Cu (001) and (111) surfaces, relative to the vacuum level. The latter surface has two types, *A* and *B*, of close-packed steps. The bulk cohesive energy of copper is -3.54 eV/atom.

Indium atom site	Crystallographic surface	
	(001)	(111) Type <i>A, B</i>
Adatomic equilibrium site	-2.94	-2.75
Top of step	-2.95	$-2.78, -2.78$
Base of step	-3.27	$-3.27, -3.26$
Kink	-3.49	$-3.49, -3.48$
Step substitutional site	-3.69	$-3.67, -3.67$
Terrace substitutional site	-3.95	-3.87

on them.

Table I lists the formation energy for an indium adatom atop the Cu surface and for an indium atom at substitutional sites in surface and near-surface layers, relative to that for indium in bulk Cu.⁴⁷ Clearly the substitutional surface site is energetically favored over the adatom site, consistent with the PAC results but contrary to the molecular-cluster calculations by Li *et al.*¹⁸ The surface site is energetically favored over bulk sites as well, consistent with the known negligible solubility of indium in copper at low temperatures.

Table II gives the binding energy for an indium atom at various sites (or traps) on the stepped Cu surfaces, relative to the vacuum level.⁴⁸ The two types of close-packed steps on the Cu (111) surface, referred to here as *A* and *B*, are illustrated in Fig. 1. There are also two distinct adatom binding sites on Cu (111) as shown in Fig. 1; an indium adatom at (fcc) site *A* lies 0.004 eV lower in energy than an adatom at (hcp) site *B*. Breeman and Boerma²⁸ obtain binding energies for indium at the Cu (001) surface rather smaller in magnitude than these, but with similar differences.

Table III gives the migration energy for an indium atom on various diffusion paths on the stepped Cu surfaces. These values are obtained by removing one degree of freedom from the motion of the indium atom and moving it incrementally along the diffusion path between two

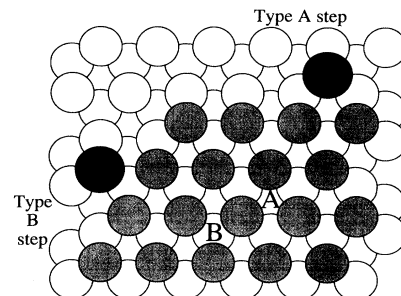


FIG. 1. Close-packed, type-*A* and type-*B* steps on the Cu (111) surface. The shaded circles are Cu atoms at surface lattice sites in the upper terrace; the open circles are Cu atoms at sites in the lower terrace and below. The two dark circles are In adatoms at trapping sites at the two types of steps. The letters *A* and *B* superposed on the upper terrace indicate the two distinct adatom binding sites on a Cu (111) terrace.

TABLE III. Migration energy (eV) of indium adatoms on stepped Cu (001) and (111) surfaces. The latter surface has two types, *A* and *B*, of close-packed steps. The asterisk indicates those migration energy values that are the difference of two binding energies (from Table II), since the diffusion path does not cross over an appreciable energy barrier.

Diffusion path	Crystallographic surface	
	(001)	(111) Type <i>A, B</i>
On terrace	0.32	0.02
On terrace by "exchange" mechanism	1.01	1.26
Down step	0.57	0.39, 0.39
Down step by "exchange" mechanism	0.65	0.44, 0.17
Along base of step	0.18	0.14, 0.25
Along base of protruding step, at kink corner	0.35	0.30, 0.33
Away from (perpendicular to) step	0.59	0.52*, 0.51*
Away from kink site, parallel to step	0.33	0.32, 0.42
Away from kink site, up the protruding step		0.51, 0.65
Away from kink site, perpendicular to step	0.58	0.74*, 0.73*

energy minima, all the while relaxing all other degrees of freedom of the system of atoms; the migration energy is then the maximum (saddle-point) total energy attained minus the initial, minimum (equilibrium) energy. The "exchange" mechanism referred to in the table is the diffusion process whereby an indium adatom displaces a Cu surface or step substitutional atom, so that the indium atom occupies that substitutional site and a Cu atom sits atop the surface as an adatom. To mimic this physical process, the displaced Cu atom is moved and the adjacent In adatom is allowed to "fall into" the vacated surface or step site.

The migration energies for diffusion by atom exchange on a terrace are so large that incorporation of an indium adatom into the Cu surface layer by the exchange mechanism is very unlikely. Incorporation of an indium adatom on an upper terrace into a descending step is energetically competitive with "jump" diffusion of the adatom down the step to the lower terrace, and the former process will in fact dominate the latter in the case of an indium adatom atop a type-*B* step on the Cu (111) surface (although Table III shows that an adatom is much more likely to diffuse to the base of an ascending step in any case).

It is noteworthy that the migration energies for indium adatom surface diffusion are somewhat smaller than those values calculated by Liu *et al.*²⁵ for copper self-diffusion by the "hopping" mechanism: 0.38 and 0.026 eV at Cu (001) and (111) surfaces, respectively. The calculated migration energy 0.32 eV for indium adatom diffusion on the Cu (001) surface compares well with the experimental values 0.28(5) eV obtained via PAC by Schatz *et al.*¹⁰ and 0.24(3) eV obtained from low-energy ion

scattering (LEIS) experiments by Breeman and Boerma.^{28,49} [The PAC value is inferred from temperature-dependent population changes; the LEIS value is possibly a lower limit since it is ascertained from the *scarcity* of adatoms observed on terraces following evaporation of energetic indium atoms onto the stepped Cu (17,1,1) substrate at temperatures 88 K and above.] By contrast, Breeman and Boerma²⁸ determine the value 0.42 eV from their embedded-atom-type calculations. It is interesting to note that the migration energy 0.31(3) eV was obtained by Fink *et al.*¹² for indium adatom diffusion over the Ag (001) surface,⁵⁰ and by Schatz *et al.*¹⁰ for indium adatom diffusion over the Ni (001) surface, in PAC experiments similar to those described here for Cu surfaces. The values in Table III agree well with the observations by Breeman and Boerma²⁸ that the migration energy of indium atoms along step edges on Cu (001) surfaces is less than 0.20 eV, and that the migration energy for indium atoms at steps diffusing past kinks is about equal to the migration energy for indium adatom diffusion over the terrace. Klas *et al.*^{8,9} infer an activation energy 0.41(3) eV for incorporation of an indium adatom at a type-*A* step on the Cu (111) surface into a step substitutional site, and an activation energy 0.64(4) eV for its subsequent incorporation into a terrace substitutional site; however, it is not clear by what mechanisms or diffusion paths these events occur.

The diffusion coefficient *D* for indium adatom diffusion over the terrace can be calculated by use of the relation proposed by Voter and Doll,⁵¹

$$D = \frac{nv l^2}{2\alpha} \exp \left[\frac{-E^a}{k_B T} \right], \quad (2)$$

TABLE IV. Binding energy (eV) of two indium atoms at terrace substitutional sites on Cu (001) and (111) surfaces. Positive values indicate that formation of the cluster is energetically unfavored.

Spatial relationship between the two sites	Crystallographic surface	
	(001)	(111)
Nearest neighbors	0.26	0.31
Next-nearest neighbors	0.03	0.03
Well separated (isolated)	0.00	0.00

where ν is the jump attempt frequency (roughly the vibrational frequency of the adatom), l is the jump distance to an adjacent site, n is the number of jump directions available to the adatom, α is the dimensionality of the space ($\alpha=2$ for typical surface diffusion), and E^a is the jump activation energy taken from Table III. The attempt frequency is computed from

$$\nu = \frac{1}{2\pi} \left[\frac{c}{m} \right]^{1/2}, \quad (3)$$

where c is the force constant ($F = -cx$) of a parabola fitted to the region near the minimum of the potential-energy curve produced by slightly displacing the adatom from its equilibrium terrace position (while allowing all other atoms to relax), and m is the indium adatom mass. This procedure gives preexponential factors 0.9×10^{-3} and $1.2 \times 10^{-4} \text{ cm}^2 \text{ s}^{-1}$ for indium adatom diffusion on Cu (001) and (111) surfaces, respectively. These values are comparable to those found for self-diffusion on various metal surfaces (see, for example, Liu *et al.*²⁵).

C. Indium clusters at surfaces

Tables IV and V show that indium clusters involving one or more indium atoms at terrace substitutional sites are not energetically favored, consistent with the notion of indium as an oversized impurity in copper. In fact, no local energy minimum exists for the case of an indium adatom at the threefold hollow site on the Cu (111) surface immediately adjacent to an indium terrace substitutional atom. Where there is more than one type of next-nearest-neighbor site, the binding energy given in the tables is that for the site producing the largest value; in no case was the binding energy negative. These positive (repulsive) binding energies conflict with the evidence from PAC experiments^{7,9} for clusters of indium atoms within the Cu (001) and (111) surface layers; with calculations by Breeman, Barkema, and Boerma²⁹ showing an attractive interaction (binding energy -0.047 eV) between substitutional indium atoms comprising a linear chain oriented in a $\langle 100 \rangle$ -type direction ("next-nearest neighbors" in Table IV) in the surface layer of Cu (001); and with the speculation by Li *et al.*¹⁸ and by Klas *et al.*⁹ that a terrace substitutional indium atom may trap indium adatoms on the Cu (001) and (111) surfaces, respectively.

The energetically favored clusters comprised of two to nine indium adatoms on the Cu (001) surface are depicted in Fig. 2. Only diagonal (or "checkerboard") adatom sites are occupied, which produces a coverage resembling

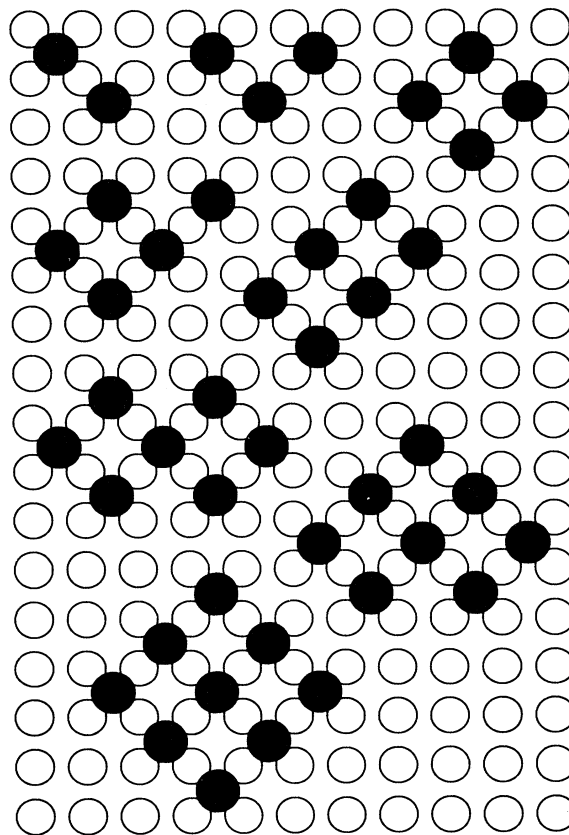


FIG. 2. Energetically favored indium adatom clusters on the Cu (001) surface. The filled and open circles represent the indium adatoms and copper terrace atoms, respectively. This surface is rotated so that the crystallographic direction [100] is diagonal on the page, and the direction [110] is vertical.

the In (001) surface. The indium atoms in a cluster relax slightly towards one another and form a tentlike structure, where those atoms at the interior of the cluster lie higher above the substrate (by a few hundredths of an angstrom) than those indium atoms at the periphery. [Larger clusters, which were not studied here, may form antiphase $c(2 \times 2)$ domains to accommodate the lattice mismatch, as has been observed for near-monolayer coverage of Pb on Cu (001) by Höslér and Moritz,⁵² Cohen *et al.*,⁵³ and others.] Figure 3 presents the cluster dissociation energy [$E_n^d = -(E_n^t + E_0^t - E_{n-1}^t - E_1^t)$, where E_n^t is the total energy of the n -adatom cluster plus Cu substrate] for the clusters shown in Fig. 2. This quantity is a

TABLE V. Binding energy (eV) of a terrace substitutional indium atom and an indium adatom on Cu (001) and (111) surfaces. Positive values indicate that formation of the cluster is energetically unfavored.

Adatom site	Crystallographic surface	
	(001)	(111)
Adjacent hollow (equilibrium) site	0.28	
Next-nearest hollow (equilibrium) site	0.01	0.00
Well separated (isolated)	0.00	0.00

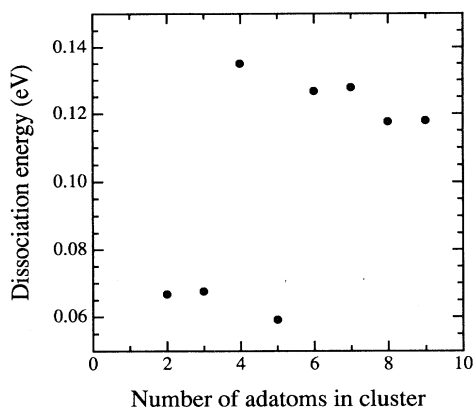


FIG. 3. Dissociation energies for the indium adatom clusters on the Cu (001) surface depicted in Fig. 2. Adatoms attached to a cluster by one or two indium-indium bonds have dissociation energies of approximately 0.06 or 0.12 eV, respectively.

rough measure of the strength of the atomic bonding at the site of the least-coordinated cluster atom. Dissociation energies of approximately 0.06 and 0.12 eV are obtained for adatoms with one and two indium-indium bonds, respectively. The cluster cohesive energy [$E_n^c = (E_n^t - E_0^t)/n$] decreases rapidly from the value -2.94 eV for a cluster comprised of a single indium adatom to the asymptotic value -3.06 eV for the complete indium $c(2 \times 2)$ monolayer coverage.

The energetically favored clusters comprised of two to six indium adatoms on the dense Cu (111) surface are depicted in Fig. 4, and the corresponding cluster dissociation energies are given in Fig. 5. The trimer is particularly stable, since the indium atom spacings are only slightly reduced from those at the In (111) surface. The lattice mismatch is evident, however, in the instability of a compact, six-atom indium cluster against dissolution into two trimers connected by a single indium-indium bond. Where larger, compact clusters are stable, the interior adatoms again lie higher above the substrate than those

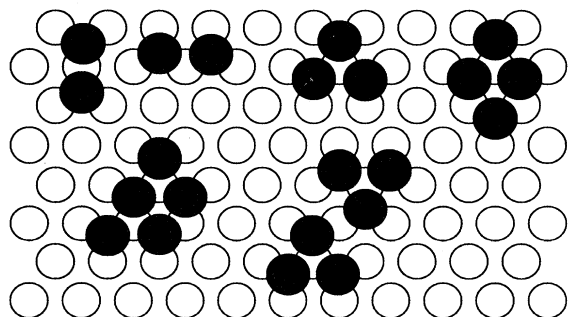


FIG. 4. Energetically favored indium adatom clusters on the Cu (111) surface. The filled and open circles represent the indium adatoms and copper terrace atoms, respectively. The first dimer shown has adatoms at surface sites *A* and *B* separated by a copper terrace atom; the second dimer has adatoms at adjacent *A* sites.

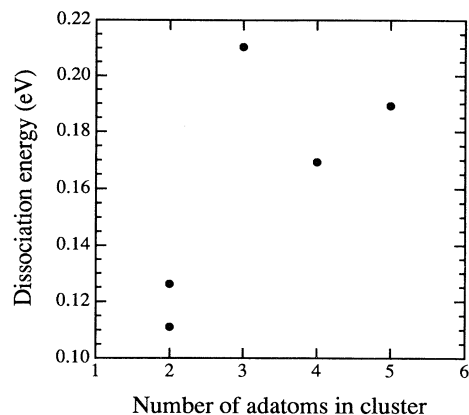


FIG. 5. Dissociation energies for the indium adatom clusters on the Cu (111) surface depicted in Fig. 4. The *A-B* dimer has a larger dissociation energy than the *A-A* dimer (and so is energetically favored), but is less mobile than the latter. The dissociation energy for a cluster is otherwise little affected by whether adatoms reside at *A* or *B* sites; for example, the *A-A* dimer is only 0.004 eV lower in energy than the *B-B* dimer, and the *A-A-A* trimer is only 0.001 eV lower in energy than the *B-B-B* trimer.

adatoms at the periphery. Dimers and trimers are found to be highly mobile, with migration energies of 0.01 and 0.05 eV, respectively, due to a “wake” effect whereby the preceding adatom pushes copper surface atoms apart and so lowers the diffusion barrier for the following adatom(s).

Indium adatoms form clusters with Cu adatoms as well. The (attractive) binding energies of In-Cu dimers on the Cu (001) and (111) surfaces are -0.31 and -0.39 eV, respectively, relative to well-separated adatoms. These values are somewhat less than the binding energies of Cu-Cu dimers, which are -0.36 and -0.44 eV, respectively. Clusters comprised primarily of Cu adatoms grow epitaxially, with the indium adatoms at the periphery of the cluster, and preferably at a cluster corner, in the lowest-energy configurations.

D. Indium clusters at steps

To obtain a good fit between Monte Carlo simulations and LEIS time-of-flight (TOF) measurements, Breeman and co-workers^{49,54} proposed that indium adatoms trapped at steps on the Cu (001) surface form rows buckled perpendicularly to the surface and to the step. By contrast, only dimers are found to be energetically favored (with binding energy of -0.01 eV, relative to two well-separated In adatoms at a step) in this work. Because the separation of the two adatoms comprising the dimer slightly exceeds the Cu-Cu nearest-neighbor separation, the adatoms reside higher above the surface than an isolated indium adatom. Thus the mobility of the dimer along the base of the step is enhanced over that of the isolated adatom. However, rather than migrate together in a coordinated fashion, the two adatoms move to adjacent surface sites in separate events. In this dimer

“dissolution-recombination” process, the migration energy for the preceding adatom is 0.12 eV and that for the following adatom is 0.11 eV, which are to be compared with the value 0.18 eV for migration of an isolated indium adatom along the step (Table III).

The dimer configuration is energetically favored for two indium adatoms at a type-*A* step on the Cu (111) surface (dimer binding energy -0.01 eV, trimer binding energy 0.05 eV), but not for adatoms at a type-*B* step (dimer binding energy 0.01 eV). Adatom diffusion along the step is enhanced in each case, however, by the dimer dissolution-recombination process. The migration energies for the preceding (following) adatoms are 0.11 eV (0.10 eV) and 0.20 eV (0.20 eV) for dimer diffusion at type-*A* and type-*B* steps, respectively. These values are to be compared with the migration energies 0.14 and 0.25 eV for isolated adatom diffusion at type-*A* and -*B* steps (Table III).

The lower migration energies for paired indium adatoms at steps on Cu (001) and (111) surfaces suggest that, despite the unfavorable energetics for “epitaxial” indium clustering at the steps, adatoms trapped there may collect in one-dimensional clusters with a high fraction of single “missing” adatoms to accommodate the lattice mismatch.

The presence of an indium atom at a step substitutional site on the Cu (001) and (111) surfaces does not initiate growth of an indium adatom cluster, as moving an indium adatom along the base of the step to an adjacent equilibrium site is found not to be energetically favorable in any case.

III. DISCUSSION

The calculated binding energies and migration energies for isolated ^{111}In probe atoms are consistent with the temperature-dependent sequence of events inferred from the PAC experiments. An indium adatom deposited on a Cu (001) or (111) surface migrates to, and is trapped at, a step on that surface. It subsequently diffuses along the base of the step until it is trapped at a kink or step vacancy. Eventually the adatom is incorporated into the upper terrace either by engulfment as the step precedes the growing terrace or by diffusion via the surface vacancy mechanism. In the former case, terrace growth occurs by

trapping of Cu adatoms at step defects; EAM calculations produce migration energies of 0.27, 0.25, and 0.29 eV for diffusion of Cu adatoms along steps on the Cu (001) surface and along type-*A* and -*B* steps on the Cu (111) surface, respectively.

Provided that a percent or more of a monolayer of indium atoms is present, one-dimensional clustering of indium adatoms at steps is likely, due, however, to reduced energy barriers for diffusion of adatom pairs rather than to significant indium-indium binding. Such irregular, mobile “clusters” may appear as buckled rows in the LEIS TOF experiments by Breeman and co-workers.^{49,54}

Formation of in-terrace, substitutional indium atom clusters is found to be highly unlikely, except where indium dimers at a step are engulfed by a growing terrace. This cannot provide the explanation for the PAC results (new in-terrace populations f'_0 and f''_0) obtained by Klas *et al.*,^{7,9} however, since they were careful to ensure that all ^{111}In probe atoms were already at (isolated) terrace substitutional sites prior to deposition of 0.07 or 0.08 ML of natural indium. A terrace substitutional ^{111}In atom was found not to bind an indium adatom or adatom cluster, but perhaps other substitutional probe-impurity configurations, for surface or interstitial impurities other than indium, are possible that would give the observed defect populations.¹⁷

The reader is reminded that the results of the total-energy calculations are sensitive to the choice of EAM embedding functions and pair interactions. In particular, the function set derived for this work gives rise to an indium-Cu-substrate interaction that dominates the indium-indium interaction, and so influences all the results for indium clustering on surfaces, at steps, and within the Cu surface layer. There appears to be no experimental evidence as yet for or against this dominance, although low-energy electron-diffraction (LEED) evidence^{52,53} does favor the adsorbate-Cu-substrate interaction in the case of a Pb monolayer on Cu (001), which may resemble indium on that surface.

ACKNOWLEDGMENTS

This work was supported in part by the EG&G Idaho Laboratory Directed Research & Development Program under DOE Idaho Field Office Contract No. DE-AC07-76ID01570.

¹R. Gomer, Rep. Prog. Phys. **53**, 917 (1990).

²See, for example, T. T. Tsong, C.-L. Chen, and J. Liu, J. Mater. Res. **4**, 1549 (1989).

³See, for example, E. Ganz, S. K. Theiss, I.-S. Hwang, and J. Golovchenko, Phys. Rev. Lett. **68**, 1567 (1992).

⁴See, for example, T. D. Pope, G. W. Anderson, K. Griffiths, P. R. Norton, and G. W. Graham, Phys. Rev. B **44**, 11 518 (1991).

⁵H.-J. Ernst, F. Fabre, and J. Lapujoulade, Phys. Rev. B **46**, 1929 (1992).

⁶T. Klas, J. Voigt, W. Keppner, R. Wesche, and G. Schatz, Phys. Rev. Lett. **57**, 1068 (1986).

⁷T. Klas, J. Voigt, W. Keppner, R. Platzer, R. Wesche, and G. Schatz, Hyperfine Interact. **34**, 577 (1987).

⁸T. Klas, R. Fink, G. Krausch, R. Platzer, J. Voigt, R. Wesche, and G. Schatz, Europhys. Lett. **7**, 151 (1988).

⁹T. Klas, R. Fink, G. Krausch, R. Platzer, J. Voigt, R. Wesche, and G. Schatz, Surf. Sci. **216**, 270 (1989).

¹⁰G. Schatz, R. Fink, K. Jacobs, U. Kohl, G. Krausch, J. Lohmüller, B. Luckscheiter, B.-U. Runge, and U. Wöhrmann, Phys. Scr. **T49**, 554 (1993).

¹¹R. Wesche, R. Fink, T. Klas, G. Krausch, R. Platzer, J. Voigt, and G. Schatz, J. Phys. Condens. Matter **1**, 7407 (1989).

¹²R. Fink, R. Wesche, T. Klas, G. Krausch, R. Platzer, J. Voigt,

- U. Wöhrmann, and G. Schatz, *Surf. Sci.* **225**, 331 (1990).
- ¹³R. Fink, B.-U. Runge, K. Jacobs, G. Krausch, J. Lohmüller, B. Luckscheiter, U. Wöhrmann, and G. Schatz, *J. Phys. Condens. Matter* **5**, 3837 (1993).
- ¹⁴G. S. Gollins, S. L. Shropshire, and J. Fan, *Hyperfine Interact.* **62**, 1 (1990).
- ¹⁵B. Lindgren, *Europhys. Lett.* **11**, 555 (1990).
- ¹⁶G. Schatz, X. L. Ding, R. Fink, G. Krausch, B. Luckscheiter, R. Platzer, J. Voigt, U. Wöhrmann, and R. Wesche, *Hyperfine Interact.* **60**, 975 (1990).
- ¹⁷E. Hunger and H. Haas, *Surf. Sci.* **234**, 273 (1990).
- ¹⁸Y. Li, M. R. Press, S. N. Khanna, P. Jena, and M. Yussouff, *Phys. Rev. B* **41**, 4930 (1990).
- ¹⁹A. F. Wells, *Structural Inorganic Chemistry*, 5th ed. (Oxford University Press, Oxford, 1984).
- ²⁰*Phase Diagrams of Indium Alloys and Their Engineering Applications*, edited by C. E. T. White and H. Okamoto, Monograph Series on Alloy Phase Diagrams Vol. 8 (ASM International, Materials Park, OH, 1992), p. 83.
- ²¹M. S. Daw and M. I. Baskes, *Phys. Rev. Lett.* **50**, 1285 (1983); *Phys. Rev. B* **29**, 6443 (1984).
- ²²S. M. Foiles, M. I. Baskes, and M. S. Daw, *Phys. Rev. B* **33**, 7983 (1986); **37**, 10378(E) (1988).
- ²³J. H. Rose, J. R. Smith, F. Guinea, and J. Ferrante, *Phys. Rev. B* **29**, 2963 (1984).
- ²⁴J. S. Nelson, E. C. Sowa, and M. S. Daw, *Phys. Rev. Lett.* **61**, 1977 (1988); J. S. Nelson, M. S. Daw, and E. C. Sowa, *Phys. Rev. B* **40**, 1465 (1989); L. Yang, T. S. Rahman, and M. S. Daw, *ibid.* **44**, 13725 (1991).
- ²⁵C.-L. Liu, J. M. Cohen, J. B. Adams, and A. F. Voter, *Surf. Sci.* **253**, 334 (1991).
- ²⁶Z.-J. Tian and T. S. Rahman, *Phys. Rev. B* **47**, 9751 (1993).
- ²⁷C.-L. Liu and J. B. Adams, *Surf. Sci.* **294**, 211 (1993).
- ²⁸M. Breeman and D. O. Boerma, *Surf. Sci.* **287/288**, 881 (1993).
- ²⁹M. Breeman, G. T. Barkema, and D. O. Boerma, *Phys. Rev. B* **49**, 4871 (1994).
- ³⁰M. W. Finnis and J. E. Sinclair, *Philos. Mag. A* **50**, 45 (1984); G. J. Ackland and V. Vitek, *Phys. Rev. B* **41**, 10324 (1990).
- ³¹A. Yokozeki and G. D. Stein, *J. Appl. Phys.* **49**, 2224 (1978).
- ³²O. Kubaschewski, E. L. Evans, and C. B. Alcock, *Metallurgical Thermochemistry*, 4th ed. (Pergamon, Oxford, 1967), p. 375.
- ³³P. Varotsos, *J. Phys. F* **18**, 595 (1988).
- ³⁴S. C. Flower, G. A. Saunders, and Y. K. Yoğurtçu, *J. Phys. Chem. Solids* **46**, 97 (1985).
- ³⁵G. Simmons and H. Wang, *Single Crystal Elastic Constants and Calculated Aggregate Properties: A Handbook*, 2nd ed. (MIT Press, Cambridge, MA, 1971), p. 114.
- ³⁶A. Seeger, *J. Phys. F* **3**, 248 (1973).
- ³⁷O. J. Kleppa, *J. Phys. Chem.* **60**, 852 (1956).
- ³⁸O. J. Kleppa, *J. Phys. Chem.* **60**, 846 (1956).
- ³⁹K. T. Jacob and C. B. Alcock, *Acta Metall.* **21**, 1011 (1973).
- ⁴⁰D. Bhattacharya and D. B. Masson, *Metall. Trans.* **5**, 1357 (1974).
- ⁴¹H. Bosse, A. Sager, W. Lühr-Tanck, and Th. Hehenkamp, *J. Phys. F* **16**, 1337 (1986).
- ⁴²W. Lühr-Tanck, H. Bosse, Th. Kurschat, M. Ederhof, A. Sager, and Th. Hehenkamp, *Appl. Phys. A* **44**, 209 (1987).
- ⁴³F. Pleiter and C. Hohenemser, *Phys. Rev. B* **25**, 106 (1982).
- ⁴⁴R. Benedek, *J. Phys. F* **17**, 569 (1987).
- ⁴⁵The lowest-energy interstitial defect configuration is a $\langle 001 \rangle$ Cu dumbbell centered on a nearest-neighbor lattice site, where the dumbbell axis is perpendicular to the (001) plane containing that lattice site and the substitutional indium atom.
- ⁴⁶H. Wollenberger, *J. Nucl. Mater.* **69&70**, 362 (1978).
- ⁴⁷The "formation energy" is simply the total energy of a specified configuration of N copper atoms and one indium atom. The relative values in Table I are thus obtained by subtracting the formation energy for N copper atoms and one indium atom arranged such that the indium atom is at a substitutional site many layers below the surface of a Cu slab (i.e., within the bulk) from the formation energy for N copper atoms and one indium atom arranged such that the In atom resides atop or at a near-surface substitutional site in a Cu slab.
- ⁴⁸The "binding energy" is the total energy of a configuration of atoms including the indium atom at a specified site minus the total energy of the configuration of atoms without the indium atom (i.e., the indium atom is removed to infinity). Then, for example, the increase in binding energy for indium at a terrace substitutional site at the Cu (001) surface over that for indium at an adatomic equilibrium site is, from Table II, $-3.95 - (-2.94) = -1.01$ eV. That is, the system energy changes by -1.01 eV when an In adatom is moved into an existing surface vacancy. Note that this binding energy difference -1.01 eV, added to the Cu (001) surface vacancy formation energy (total energy of N copper atoms arranged in a slab with one surface vacancy minus the total energy of N copper atoms arranged in a slab with no surface vacancy; calculated to be 0.58 eV), equals the difference in formation energy for indium at terrace substitutional and adatomic sites taken from Table I, $-0.82 - (-0.39) = -0.43$ eV.
- ⁴⁹M. Breeman and D. O. Boerma, *Phys. Rev. B* **46**, 1703 (1992).
- ⁵⁰EAM calculations using the function set for indium discussed here and the Ag function set from Ref. 22 give the migration energy 0.39 eV for diffusion of an indium adatom over the Ag (001) surface. The migration energy for an indium adatom on the Ag surface is expected to be larger than that for an indium adatom on the Cu surface, due to the higher chemical reactivity of indium with Ag.
- ⁵¹A. F. Voter and J. D. Doll, *J. Chem. Phys.* **80**, 5832 (1984).
- ⁵²W. Höslér and W. Moritz, *Surf. Sci.* **175**, 63 (1986).
- ⁵³C. Cohen, Y. Girard, P. Leroux-Hugon, A. L'Hoir, J. Moulin, and D. Schmaus, *Europhys. Lett.* **24**, 767 (1993).
- ⁵⁴M. Breeman, G. Dorenbos, and D. O. Boerma, *Nucl. Instrum. Methods Phys. Res. Sect. B* **64**, 64 (1992).

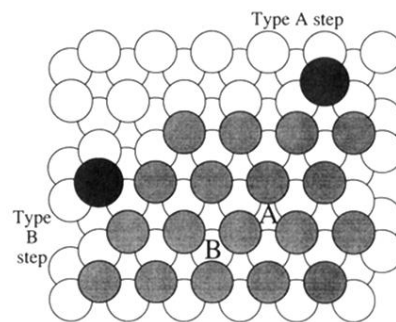


FIG. 1. Close-packed, type-*A* and type-*B* steps on the Cu (111) surface. The shaded circles are Cu atoms at surface lattice sites in the upper terrace; the open circles are Cu atoms at sites in the lower terrace and below. The two dark circles are In adatoms at trapping sites at the two types of steps. The letters *A* and *B* superposed on the upper terrace indicate the two distinct adatom binding sites on a Cu (111) terrace.